Thermoelectric Properties of Sr1-3x/2Lax/2Smx/2TiO3-δ (0.05 ≤ x ≤ 0.30) Ceramics

Adindu C. Iyasara (acnnayerugo@gmail.com)
School of Industrial Technology

Research Article

Keywords: Sr-vacancy, thermoelectric, carrier concentration, thermal conductivity, figure of merit

Posted Date: July 27th, 2021

DOI: https://doi.org/10.21203/rs.3.rs-738255/v1

Thermoelectric properties of $Sr_{1-3x/2}La_{x/2}Sm_{x/2}TiO_{3-\delta}$ ($0.05 \leq x \leq 0.30$) ceramics

Adindu C. Iyasara

School of Industrial Technology

Department of Ceramic and Glass Technology

Akanu Ibiam Federal Polytechnic Unwana, Nigeria.

Email: acnnayerugo@gmail.com

Abstract

Influence of strongly reducing processing atmosphere on Sr-vacancy $Sr_{1-3x/2}La_{x/2}Sm_{x/2}TiO_{3-\delta}$ (x = 0.05, 0.10, 0.15, 0.20, 0.30) ceramics was investigated. The ceramic powders were prepared by the solid-state reaction (SSR) method, and heat treated in 5 % H_2/N_2 reducing gas at 1573 K for 6 h and 1773 K for 8 h for calcination and sintering processes, respectively. Thermoelectric properties of $Sr_{1-3x/2}La_{x/2}Sm_{x/2}TiO_{3-\delta}$ ceramics were evaluated from 573 to 973 K. Their electrical conductivities increased with carrier concentration and also decreased with temperature, indicating metallic behaviour. The Seebeck coefficients showed n-type behaviour and increased with temperature. Additionally, the total thermal conductivities exhibited low values, with a minimum value, 2.67 W/m. K for x = 0.20 ceramics at 973 K. A maximum thermoelectric figure of merit, ZT = 0.30 at 973 K was reached for $Sr_{0.7}La_{0.1}Sm_{0.1}TiO_{3-\delta}$ ceramics, which is 20 % higher than the maximum value reported previously for La-Sm electron doped $SrTiO_3$ ceramics.

Keywords: Sr-vacancy, thermoelectric, carrier concentration, thermal conductivity, figure of merit

1. Introduction

Thermoelectric (TE) oxide ceramics have been regarded as promising materials for power generation and energy harvesting particularly at high temperatures. Oxides generally are inert, nontoxic, cheap, abundant, thermally stable, resistant to oxidation with a corresponding high temperature, hence potential TE materials for high temperature applications [1], [2]. The efficiency of a TE device such as thermoelectric power generator

(TEG) depends on the properties of the TE materials which is determined using the dimensionless figure of merit, ZT. This measuring parameter is defined as $ZT = \frac{S^2\sigma T}{k}$, where S is a Seebeck coefficient (μV/K), σ is an electrical conductivity (S/cm), T is an absolute temperature (K), and k is a thermal conductivity (W/m K^2). Therefore, for a high ZT to be achieved, a high power factor, PF ($S^2\sigma$) and a low k are required [3], [4].

State of-the-art TE materials (conventional non-oxides) e.g., PbTe/Se, Bi_2Te_3/Se_3, GeTe, etc. are toxic, scarce, expensive and unstable at high temperatures [5]. Due to their complex structures, they possess low phonon group velocity, leading to low k and optimised ZT values (ZT ≥1) [6]–[8]. However, a ZT = 1 is regarded as a performance benchmark for viable TE materials in the thermoelectrics community [9].

Despite the potential TE characteristics possessed by oxides, they exhibit high k, which leads to low ZT (particularly n-type oxides) when compared to conventional non-oxides. Several n-type oxide materials such as $SrTiO_3$, ZnO, $CaMnO_3$ and In_2O_3 have been studied. For example, high ZT values of 0.47 at 1000 K [10], [11] and 0.65 at 1247 K [10], respectively have been reported for n-type Al-Ga co-doped ZnO and recently ZT ≥ 0.6 at 1000 – 1100 K for La-Nb co-doped $SrTiO_3$ [12]. Doped and reduced $SrTiO_3$ ceramics have recently shown improved electrical conductivity required for TE applications [13]. There are various approaches such as doping, co-doping, addition/inclusions, enhanced processing condition, defect and micro/nanostructural engineering so far utilized for optimizing the TE performance of $SrTiO_3$ [14], [15].

In our previous publication [16] a maximum ZT value of 0.24 at 873 K and a minimum k = 3.0 W/m. K for x = 0.2 at 973 K were obtained for electron La-Sm co-doped $SrTiO_3$ ceramics. It is therefore established that electron co-doping had a minimal effect on thermal conductivity, hence unsuitable for optimizing ZT. In furtherance to the works reported independently by Kovalevsky *et al* [14] and Lu *et al* [17], it is agreed that batched stoichiometries with cation vacancies followed by processing in reducing atmosphere are milestone in achieving improved thermoelectric properties. This projection informs the aim of this study. It is therefore, an attempt to improve the TE properties of Sr-site vacancy La-Sm co-doped $SrTiO_3$ ceramics compared to the previous published electron doped mechanism [16].

2. Materials and method

$Sr_{1-3x/2}La_{x/2}Sm_{x/2}TiO_3$ (x = 0.05, 0.1, 0.15, 0.2, 0.3) ceramics were prepared by a solid-state reaction (SSR) method. The starting materials of $SrCO_3$ (99.90 %; Sigma-Aldrich, UK), TiO_2 (99.90 %; Sigma-Aldrich), La_2O_3 (99.99 %; Sigma-Aldrich), and Sm_2O_3 (99.90 %; Stanford Materials Corporation, USA) were mixed for 24 h with isopropanol and 10 mm diameter yttria-stabilized zirconia balls using a ball mill. The mixtures were dried at 80 ^oC for several hours and sieved using a 250 μm sieve mesh. The sieved powders were calcined in 5%H_2/N_2 gas at 1573 K for 6 h and then pressed by a uniaxial press into a 20 mm disc pellet (≤ 2mm thickness). Sintering of the pellets was performed in flowing 5%H_2/N_2 reducing gas at 1773 K for 8 h. Phases of $Sr_{1-3x/2}La_{x/2}Sm_{x/2}TiO_3$ ceramics were analyzed by x-ray diffraction (XRD) method with a D2 phaser diffractometer (Bruker AXS GmbH, Germany) using Cu Kα1 radiation with λ =1.5406 Å. Secondary electron (SE) surface images of the ceramics were also observed with a Scanning Electron Microscope (Philips XL 30 S-FEG). Seebeck coefficient and electrical conductivity of the sintered disc pellets were simultaneously measured using a NETZSCH SBA 458 NEMESIS instrument in argon atmosphere from 573 – 973 K. The thermal conductivity was determined using a thermal properties analyzer (Anter Flashline TM 3000) while the experimental density was determined by Archimedes' method using an electronic digital density balance (Mettler-Toledo AG Balance).

3. Results and discussion

XRD patterns for $Sr_{1-3x/2}La_{x/2}Sm_{x/2}TiO_3$ ($0.05 \leq x \leq 0.3$) ceramics are shown in Figure 1. All samples are single phase and indexed with the SrTiO3 cubic perovskite structure (pm-3m space group). The lattice parameters were calculated from the XRD data and the results together with relative densities measured by Archimedes' method are listed in Table 1. The lattice parameters for x = 0.05 – 0.2 ceramics increase with increasing dopant (La-Sm) concentrations with values ranging from 3.899 to 3. 91 Å, and decreases for x = 0.3 (3.902 Å). The increase in lattice parameter is attributed to a decrease in the binding energy within the lattice due to formation of oxygen vacancy and partial reduction of Ti^{4+} ions to Ti^{3+} ions [18]. Structural transitions or distortions and

solid solution limit contribute to the decrease in lattice parameter for x = 0.3 ceramics. However, the lattice parameter trend in this work is contrary to the obtained results in our previously studied electron La-Sm co-doped $SrTiO_3$ ceramics [16] and in La-Yb co-doped $SrTiO_3$ [19].

Table 1. List of Lattice parameters, cell volumes and relative densities of $Sr_{1-3x/2}La_{x/2}Sm_{x/2}TiO_3$; $0.05 \leq x \leq 0.30$ ceramics sintered in 5% H_2/N_2 gas at 1773 K for 8 h.

Composition x	Lattice parameter (Å)	Cell volume (Å)	Relative density (%)
0.05	3.899	59.273	98.1
0.10	3.906	59.593	96.1
0.15	3.907	59.639	99.1
0.20	3.91	59.776	98.7
0.30	3.902	59.41	98.2

The relative densities of all ceramics are higher than 96% and higher than most rare earth (RE) doped $SrTiO_3$ ceramics [20], [21]. The results of microstructure analysis as shown in Figure 2 are identical to the XRD results since no second phases were identified. Therefore, all microstructural images are homogeneous and dense, hence agree with their high relative densities. In addition, these SEM images showed regular polygonal-shaped grain structures while the average grain size increased with increasing doping level. Hence, the average grain size of the ceramics increased from 7.5 μm to 10.4, 10.8 and 11.2 μm for x = 0.10, 0.15, 0.20, and 0.30, respectively. Comparative analysis shows that these grain sizes are small, and evidenced by the adopted highly reducing processing conditions. This assertion is supported by in the literature where a La-Nb co-doped ceramics sintered in air exhibited a larger grain size than the same composition sintered in reducing atmosphere [15]. Reduced grain size implies an incorporation of large grain boundaries which are effective scattering centres for phonons [22]

Temperature dependencies of an electrical conductivity and an absolute Seebeck coefficient for $Sr_{1-3x/2}La_{x/2}Sm_{x/2}TiO_3$ ($0.05 \leq x \leq 0.30$) ceramics are shown in Figure 3. Electrical conductivities for all samples showed a temperature dependence of a degenerate semiconductor or metallic behaviour [23]. As shown in Figure 3a, the electrical conductivity for x = 0.30 ceramic was higher than all other compositions withing the measured temperature range. The reason for the maximum electrical conductivity can be explained by increase of the carrier concentration [9]. High dopant (La^{3+} and Sm^{3+} ions) level substituted into Sr^{2+} sites could contribute to an electrical conductivity of the doped $SrTiO_3$ ceramics. Consequently, the maximum electrical conductivity of the ceramics was 1023 S/cm at 573 K for the x = 0.30 composition.

Figure 3b shows the absolute Seebeck coefficients for $Sr_{1-3x/2}La_{x/2}Sm_{x/2}TiO_3$ ceramics. Seebeck coefficients of all compositions showed negative for whole temperature range, indicating n-type and increased with temperature, hence an exhibition of metallic behaviour [19]. Generally, a Seebeck coefficient is inversely proportional to a carrier concentration [24]. Accordingly, an increase in carrier concentration (dopant level) for these doped ceramics led to the observed decrease in Seebeck coefficients. However, the average absolute Seebeck coefficients (158 – 255 μV/K) attained in this work at high temperature (973 K) exceeds the minimum recommended Seebeck coefficient s (150 – 250 μV/K) for a potential thermoelectric materials [25].

Figure 4 represents the temperature dependencies of a total thermal conductivity and a thermoelectric figure of merit for $Sr_{1-3x/2}La_{x/2}Sm_{x/2}TiO_3$ ceramics. Total thermal conductivity for $x \leq 0.15$ and x = 0.30 ceramics decreased with increasing temperature up to 873 K, and exhibited an abnormal behaviour at high temperature (973 K). The anomaly can be explained by the concept of normal process or scattering (N-process) where momentum is conserved, leading to an increase in thermal conductivity with temperature [26]. x = 0.20 ceramics showed the lowest total thermal conductivity, and decreased with increasing temperature in the whole measurement temperature range. This trend indicates an Umklapp phonon scattering behaviour [12], [27]. Overall, a minimum total conductivity, 2.67 W/m. K at 973 K was observed for x = 0.2 ceramics, comparable to those of doped $SrTiO_3$ prepared by conventional methods [28], [29] and enhanced techniques [30], [31] The low thermal conductivity obtained indicates an application of reducing atmosphere in all heat treatments (calcination

and sintering) has an efficient impact in the thermal properties of SSR synthesized $Sr_{1-3x/2}La_{x/2}Sm_{x/2}TiO_3$ ceramics.

ZT values of ceramics increased with an increase in the dopant level up to x = 0.2 (Figure 4b) and levels off at x = 0.30. x = 0.20 ceramics maintained a leading high ZT over the whole measured temperature range, and reached a maximum ZT value of 0.30 at 973 K. This high ZT could be linked to its high lattice parameter and consequent low thermal conductivity.

Conclusions

The influence of strong reducing processing atmosphere and the effect of Sr (cation) vacancy on $Sr_{1-3x/2}La_{x/2}Sm_{x/2}TiO_3$ ($0.05 \leq x \leq 0.30$) ceramics have been studied. Ceramics were prepared by the reduced SSR method, and their thermoelectric properties were investigated from 573 – 973 K temperature range. The results obtained showed that $Sr_{1-3x/2}La_{x/2}Sm_{x/2}TiO_3$ ceramics were optimised compared to our previously reported electron doped La-Sm doped $SrTiO_3$ ($Sr_{1-x}La_{x/2}Sm_{x/2}TiO_3$) ceramics. In $Sr_{1-x}La_{x/2}Sm_{x/2}TiO_3$ ceramics, a highest ZT = 0.24 at 873 K for x = 0.15 was achieved [16] while an optimised ZT value of 0.30 was reported for $Sr_{1-3x/2}La_{x/2}Sm_{x/2}TiO_3$ (x = 0.20) ceramics in this work. The minimum total thermal conductivity (2.67 W/m. K) obtained that led to the high ZT was attributed to the creation of Sr-site vacancies and oxygen vacancies resulting from the strongly reducing processing conditions.

- AUTHOR INFORMATION

School of Industrial Technology, Department of Ceramic and Glass Technology

Akanu Ibiam Federal Polytechnic Unwana, Nigeria.

Tel: +2348124317117, Email: acnnayerugo@gmail.com

Notes The author declares no competing financial interest.

- ACKNOWLEDGMENTS

Financial support from TETFUND Nigeria is greatly acknowledged. I would also like to acknowledge the technical work (experiment) – XRD, SEM and thermoelectric characterization carried out at the functional materials and devices laboratory and the Sorby centre, department of Materials Science and Engineering, the University of Sheffield, UK.

References

[1] A. C. Iyasara, F. U. Idu;, E. O. Nwabineli;, T. C. Azubuike;, and C. . Arinze, "Thermoelectric Study of $La_2Ti_{2-x}Nb_xO_7$ ($0 \leq x \leq 0.25$) Ceramic Materials," *J. Energy Res. Rev.*, vol. 6, no. 4, pp. 38–47, 2020, doi: 10.1002/9781118407899.ch6.

[2] K.-H. Jung, S.-M. Choi, C.-H. Lim, W.-S. Seo, and H.-H. Park, "Phase analysis and thermoelectric properties of Zn1−xMxO (M= Al, Ga) samples," *Surf. Interface Anal.*, vol. 44, no. 11–12, pp. 1507–1510, 2012.

[3] T. M. Tritt and M. A. Subramanian, "Thermoelectric Materials, Phenomena, and Applications : A Bird' s Eye View," *MRS Bull.*, vol. 31, no. March, pp. 188–198, 2006, doi: 10.1557/mrs2006.44.

[4] D. Nemir and J. Beck, "On the significance of the thermoelectric figure of merit Z," *J. Electron. Mater.*, vol. 39, no. 9, pp. 1897–1901, 2010, doi: 10.1007/s11664-009-1060-4.

[5] J. T. Jarman, E. E. Khalil, and E. Khalaf, "Energy Analyses of Thermoelectric Renewable Energy Sources," *Open J. Energy Effic.*, vol. 02, no. 04, pp. 143–153, 2013, doi: 10.4236/ojee.2013.24019.

[6] G. Kieslich *et al.*, "A chemists view: Metal oxides with adaptive structures for thermoelectric applications," *Phys. Status Solidi Appl. Mater. Sci.*, vol. 213, no. 3, pp. 808–823, 2016, doi: 10.1002/pssa.201532702.

[7] G. J. Snyder and E. S. Toberer, "Complex thermoelectric materials," *Nat Mater*, vol. 7, no. 2, pp. 105–114, 2008, doi: 10.1038/nmat2090.

[8] H. J. Goldsmid, *Introduction to Thermoelectricity*. Springer Series in materials science 121, 2010.

[9] J. He, Y. Liu, and R. Funahashi, "Oxide thermoelectrics: The challenges, progress, and outlook," *J. Mater. Res.*, vol. 26, no. 15, pp. 1762–1772, 2011, doi: 10.1557/jmr.2011.108.

[10] M. Košir, M. Podlogar, N. Daneu, A. Rečnik, E. Guilmeau, and S. Bernik, "Phase formation, microstructure development and thermoelectric properties of $(ZnO)_kIn_2O_3$ceramics," *J. Eur. Ceram. Soc.*, vol. 37, no. 8, pp. 2833–2842, 2017, doi: 10.1016/j.jeurceramsoc.2017.03.019.

[11] M. Ohtaki, K. Araki, and K. Yamamoto, "High thermoelectric performance of dually doped ZnO ceramics," *J. Electron. Mater.*, vol. 38, no. 7, pp. 1234–1238, 2009, doi: 10.1007/s11664-009-0816-1.

[12] J. Wang *et al.*, "Record high thermoelectric performance in bulk $SrTiO_3$ via nano-scale modulation doping," *Nano Energy*, vol. 35, no. April, pp. 387–395, 2017, doi: 10.1016/j.nanoen.2017.04.003.

[13] J. A. Dawson, X. Li, C. L. Freeman, J. H. Hardinga, and D. C. Sinclair., "The application of a new potential model to the rare-earth doping of $SrTiO_3$ and $CaTiO_3$," *J. Mater. Chem. C*, vol. 1, no. 8, pp. 1574–1582, 2013, doi: 10.1039/c2tc00475e.

[14] A. V. Kovalevsky *et al.*, "Designing strontium titanate-based thermoelectrics: insight into defect chemistry mechanisms," *J. Mater. Chem. A*, vol. 5, no. 8, pp. 3909–3922, 2017, doi: 10.1039/C6TA09860F.

[15] D. Srivastava *et al.*, "Tuning the Thermoelectric Properties of A-site Deficient $SrTiO_3$ Ceramics by Vacancies and Carrier Concentration," *Phys. Chem. Chem. Phys.*, vol. 18, pp. 26475–26486, 2016, doi: 10.1039/C6CP05523K.

[16] A. C. Iyasara, W. L. Schmidt, R. Boston, D. C. Sinclair, and I. M. Reaney, "La and Sm Co-doped $SrTiO_{3-\delta}$ Thermoelectric Ceramics," in *Materials Today: Proceedings*, 2017, vol. 4, no. 12, doi: 10.1016/j.matpr.2017.10.004.

[17] Z. Lu, H. Zhang, W. Lei, D. C. Sinclair, and I. M. Reaney, "High-Figure-of-Merit Thermoelectric La-Doped A-Site-Deficient SrTiO3 Ceramics," *Chem. Mater.*, vol. 28, no. 3, pp. 925–935, 2016, doi: 10.1021/acs.chemmater.5b04616.

[18] D. Neagu and J. T. S. Irvine, "Structure and Properties of $La_{0.4}Sr_{0.4}TiO_3$ Ceramics for Use as Anode

Materials in Solid Oxide Fuel Cells," *Chem. Mater.*, vol. 22, no. 6, pp. 5042–5053, 2010, doi: 10.1021/cm101508w.

[19] H. Wang and C. Wang, "Thermoelectric properties of Yb-doped $La_{0.1}Sr_{0.9}TiO_3$ ceramics at high temperature," *Ceram. Int.*, vol. 39, no. 2, pp. 941–946, 2013, doi: 10.1016/j.ceramint.2012.07.009.

[20] H. C. Wang *et al.*, "Enhancement of thermoelectric figure of merit by doping Dy in $La_{0.1}$ $Sr_{0.9}$ TiO_3 ceramic," *Mater. Res. Bull.*, vol. 45, no. 7, pp. 809–812, 2010, doi: 10.1016/j.materresbull.2010.03.018.

[21] J. Liu *et al.*, "Thermoelectric properties of Dy-doped $SrTiO_3$ ceramics," *J. Electron. Mater.*, vol. 41, no. 11, pp. 3073–3076, 2012, doi: 10.1007/s11664-012-2219-y.

[22] R. Boston *et al.*, "Protocols for the fabrication, characterization, and optimization of n-type thermoelectric ceramic oxides," *Chem. Mater.*, vol. 29, no. 1, pp. 265–280, 2017, doi: 10.1021/acs.chemmater.6b03600.

[23] H. C. Wang *et al.*, "Doping effect of La and Dy on the thermoelectric properties of $SrTiO_3$," *J. Am. Ceram. Soc.*, vol. 94, no. 3, pp. 838–842, 2011, doi: 10.1111/j.1551-2916.2010.04185.x.

[24] T. M. Tritt, "Thermoelectric Materials : Principles , Structure , Properties , and Applications," *Encycl. Mater. Sci. Technol.*, pp. 1–11, 2002, doi: http://dx.doi.org/10.1016/B0-08-043152-6/01822-2.

[25] A. M. Dehkordi, "An Experimental Investigation Towards Improvement of Thermoelectric Properties of Strontium Titanate Ceramics," Clemson University, 2014.

[26] D. Spiteri, "Understanding phonon scattering and predicting thermal conductivity from molecular dynamics simulation," University of Bristol, 2015.

[27] W. Li, S. Lin, X. Zhang, Z. Chen, X. Xu, and Y. Pei, "Thermoelectric Properties of Cu_2SnSe_4 with Intrinsic Vacancy," *Chem. Mater.*, vol. 28, no. 17, pp. 6227–6232, 2016, doi: 10.1021/acs.chemmater.6b02416.

[28] A. V. Kovalevsky *et al.*, "Towards a high thermoelectric performance in rare-earth substituted $SrTiO_3$: effects provided by strongly-reducing sintering conditions," *Phys. Chem. Chem. Phys.*, vol. 16, no. 48, pp. 26946–26954, 2014, doi: 10.1039/C4CP04127E.

[29] J. Liu *et al.*, "Influence of rare earth doping on thermoelectric properties of $SrTiO_3$ ceramics," *J. Appl. Phys.*, vol. 114, no. 22, 2013, doi: 10.1063/1.4847455.

[30] D. Ekren *et al.*, "Enhancing the thermoelectric power factor of $Sr_{0.9}Nd_{0.1}TiO_3$ through control of the nanostructure and microstructure," *J. Mater. Chem. A*, vol. 6, no. 48, pp. 24928–24939, 2018, doi: 10.1039/c8ta07861k.

[31] D. Srivastava, C. Norman, F. Azough, M. C. Schäfer, E. Guilmeau, and R. Freer, "Improving the thermoelectric properties of $SrTiO_3$-based ceramics with metallic inclusions," *J. Alloys Compd.*, vol. 731, no. January, pp. 723–730, 2018, doi: 10.1016/j.jallcom.2017.10.033.

Figures

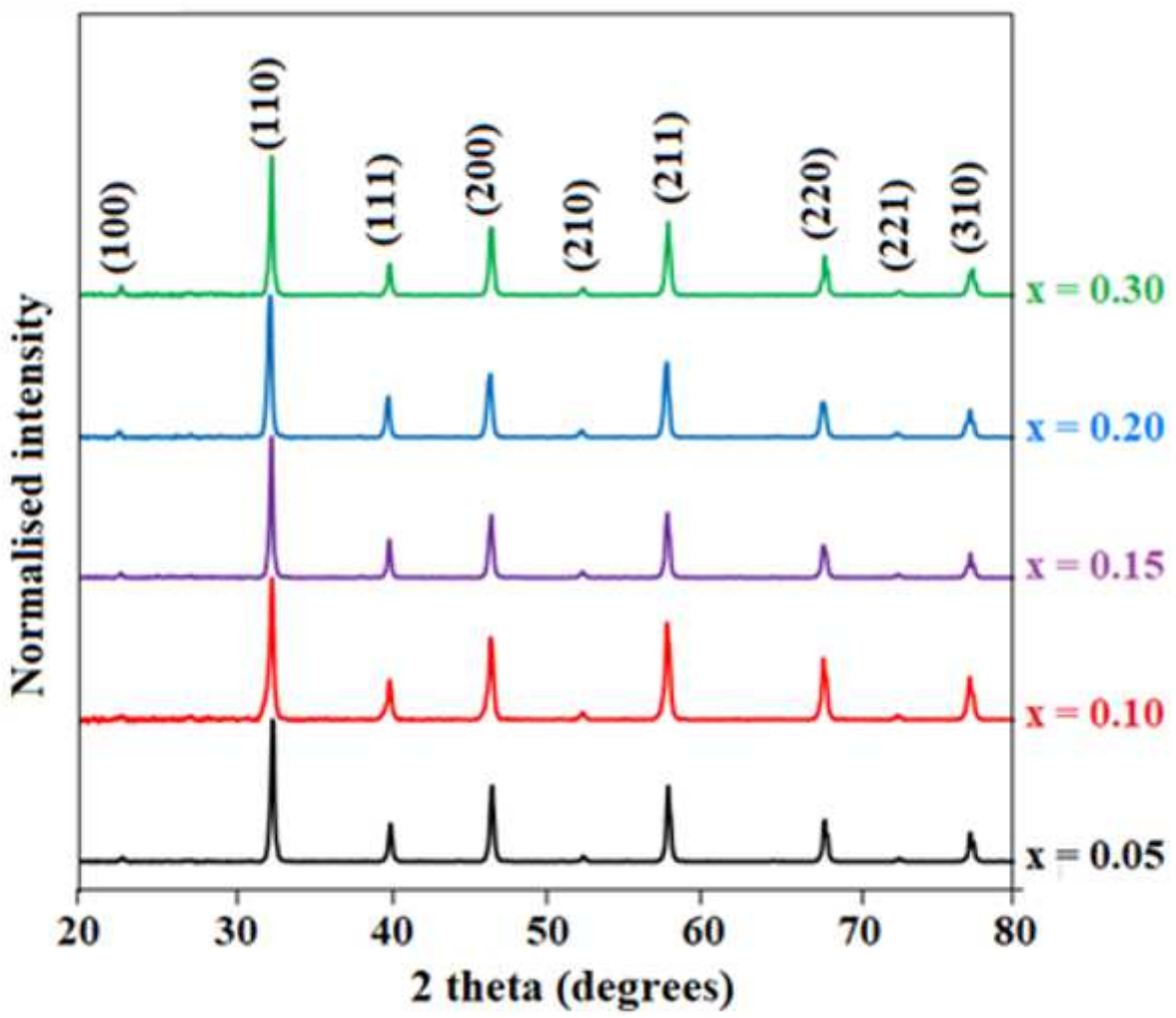

Figure 1

XRD analysis results for Sr1-3x/2Lax/2Smx/2TiO3 (0.05 ≤ x ≤ 0.3) ceramics sintered in 5%H2/N2 gas at 1773 K for 8 h.

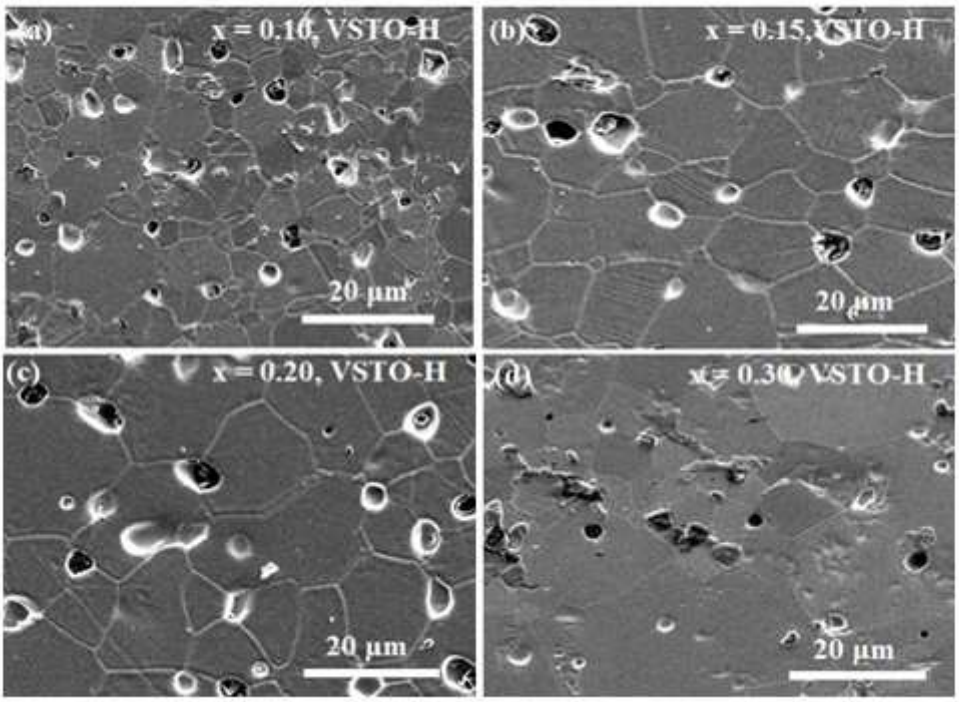

Figure 2

SEM images of the surfaces for Sr1-3x/2Lax/2Smx/2TiO3 (x = 0.05, 0.15, 0.20, 0.30) ceramics sintered in 5% H2/N2 at 1773 K for 8 h.

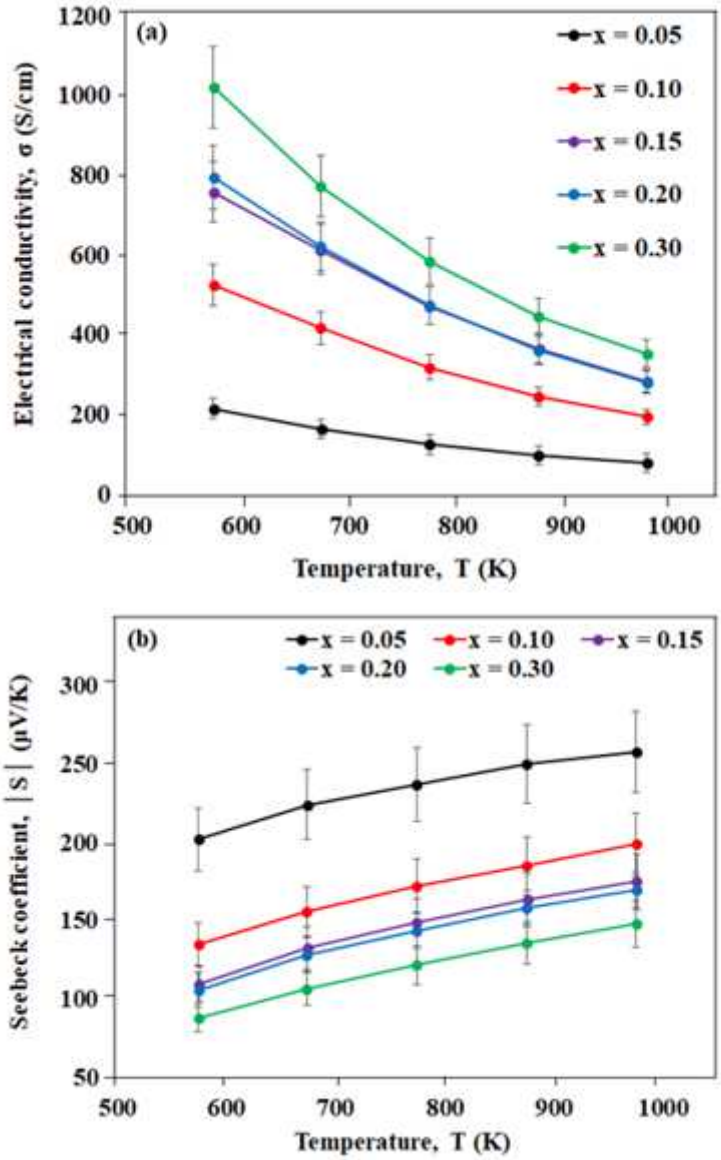

Figure 3

Temperature dependencies of (a) electrical conductivities and (b) absolute Sebeck coefficients for Sr1-3x/2Lax/2Smx/2TiO3 (0.05 ≤x ≤ 0.30) ceramics sintered in 5% H2/N2 at 1773 K for 8 h.

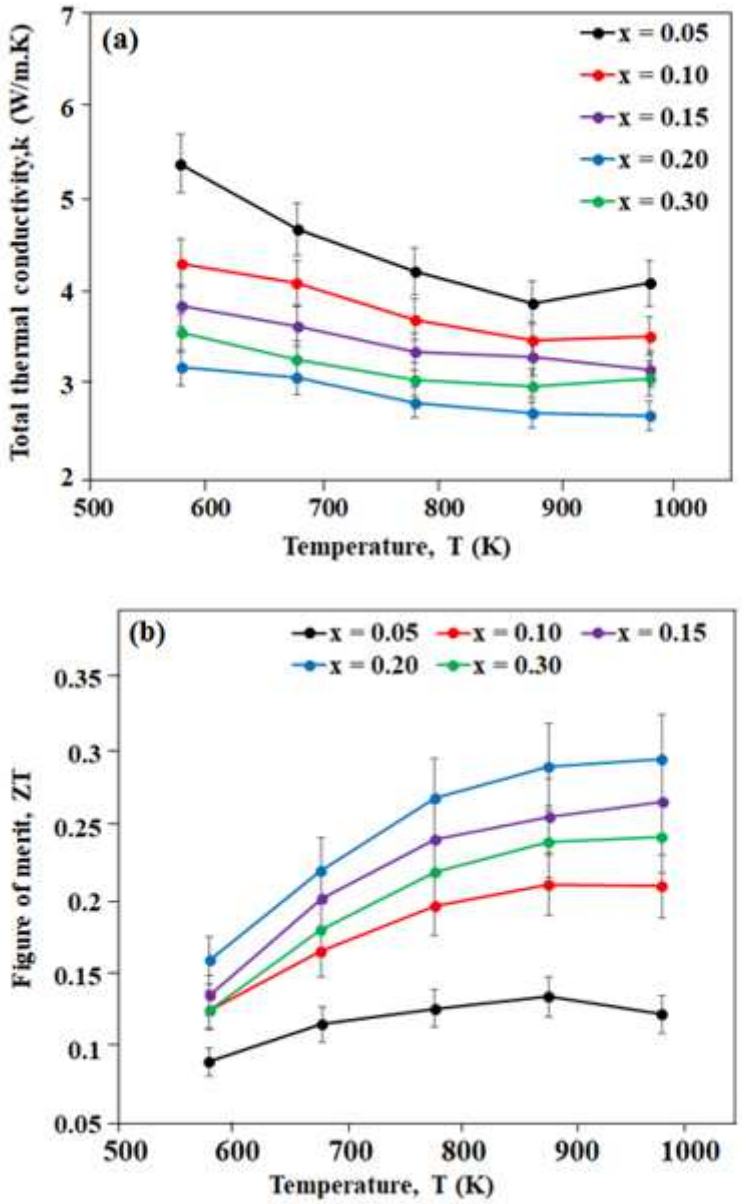

Figure 4

Temperature dependencies of (a) total thermal conductivities and (b) thermoelectric figure of merit for Sr1-3x/2Lax/2Smx/2TiO3 (0.05 ≤x ≤ 0.30) ceramics sintered in 5% H2/N2 at 1773 K for 8 h.